Performance Evaluation of a Fast Computation Algorithm for the DMT in High-Speed Subscriber Loop

Inkyu Lee, *Student Member, IEEE*, Jacky S. Chow, *Member, IEEE*, and John M. Cioffi, *Senior Member, IEEE*

***Abstract*—The discrete multitone (DMT) modulation is considered to be a viable transmission scheme for high-speed subscriber loop. In this paper, the fast algorithm for computing the equalizer settings derived in [1] is extended and applied for the DMT in high-speed subscriber loop. The channel pulse response is assumed to be given by the channel identification method, and then the equalizer filter settings are computed. In simulations, a fast algorithm for the symbol spaced equalizer in a colored noise channel is used. Simulation results performed in various CSA loops indicate that the fast algorithm yields the near-optimum settings for the DMT system.**

I. Introduction

THERE HAS been growing interest in utilization of existing unshielded copper twisted pair for various applications including but not limited to ISDN, DSL, HDSL, and more recently, ADSL. The maximum achievable data rate on the carrier serving area (CSA) loops, containing approximately 80% of the lines between central offices (CO) and remote customer premises, has been improving and has exceeded 6 Mbps for ADSL application.

This paper describes the discrete multitone (DMT) modulation in high-speed subscriber loop. DMT modulation has been chosen as the ANSI standard for data transmission for ADSL application.

The receiver of a DMT system consists of a time-domain equalizer (TEQ) that is an FIR filter and there are several methods to train the TEQ during startup, see [2] and [3]. However, these methods either involve intense computation such as matrix inversion [2], or require a significant amount of iterations and time before the algorithm reaches convergence [3]. The former method thus results in high complexity count and expensive cost, and the latter method may have limited applications, especially in areas where a fast training time is crucial.

In most practical situations, the channel response is not known *a priori*. Thus adaptation of the equalizer is essential when data is transmitted over an unknown channel. As discussed in [1], the conventional LMS algorithm of the TEQ may take millions of iterations to converge to the optimal settings on a copper twisted pair loop channel.

The slow convergence motivates study of non-iterative methods to compute the optimum equalizer settings. Thus, in contrast to the conventional recursive adaptive technique, Lee and Cioffi [1] have proposed the fast computation algorithm of the decision feedback equalizer (DFE) that has a similar structure to the TEQ. Exploiting this structural similarity, this paper extends the non-recursive fast algorithm in [1] to the TEQ case and examines performance of the non-recursive fast algorithm in high-speed subscriber loop.

Non-iterative adaptive algorithm proposed in [1] is based on the channel estimates. The equalizer coefficients are computed using the discrete Fourier transform (DFT) operation very efficiently. Since the Toeplitz autocorrelation matrices are approximated by the circulant matrices, the solution from the fast algorithm is not exactly the optimum solution. However, the SNR difference from the exact solution is only a few tenth of a dB. Moreover, the gap approaches zero as the size of the autocorrelation matrix (the length of the feedforward filter, in the TEQ case) increases, since a circulant matrix is asymptotically equivalent to a Toeplitz matrix [4].

The fast algorithm is attractive especially in the DMT scheme since the fast Fourier transform (FFT) operation embedded in the DMT can be shared to generate the solution of the fast algorithm without costing additional hardware.

In this paper, the channel pulse response is assumed to be given using some well-known channel identification techniques. This identification can be done in a few thousand iterations and still takes much shorter time in comparison with the total convergence time of the conventional LMS algorithm. When noise is no longer white, the noise autocorrelation function can also be estimated with a little longer training sequences. Channel identification problem will be described later.

We will show that the proposed fast algorithm computes the TEQ coefficients with much reduced complexity compared with the method in [2] and obtains the results with a much shorter time period than the method described in [3] even after taking into account the process of channel identification.

In Section II, the DMT structure is explained and the TEQ is described in more detail. Section III briefly shows the optimum TEQ settings [2]. The only difference between the TEQ and the DFE is that the minimum phase constraint on the feedback

Manuscript received February 10, 1995; revised May 12, 1995. This work was supported by a gift from Samsung, Korea and by NSF under Contract NCR-9203131.

I. Lee and J. M. Cioffi are with the Information Systems Laboratory, Stanford University, Durand 112, Stanford, CA 94305 USA.

J. S. Chow is with the Amati Communications Corporation, Mountain View, CA 94040 USA.

IEEE Log Number 9415201.

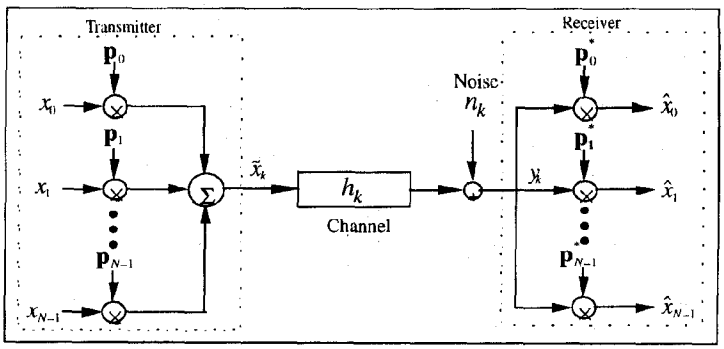

Fig. 1. Basic structure of a DMT system.

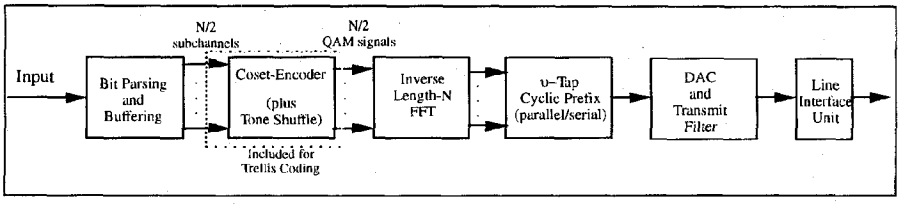

Fig. 2. Block diagram of a DMT transmitter.

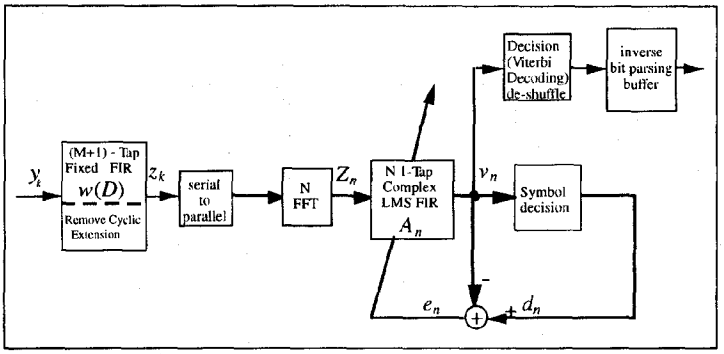

Fig. 3. Block diagram of a DMT receiver.

filter is not required in the TEQ. Thus, the DFE is a special case of the TEQ solution with a minimum-phase constraint on the feedback filter. The computation of the TEQ coefficients can be easily extended from the DFE case by changing the position of a unit center tap in the feedback filter. (In the DFE, the position of a unit center tap is set to the first tap.)

In Section IV, we revisit the fast algorithm with a colored noise case. Section V briefly discusses the channel identification problem. Finally, Section VI shows the simulation results for various copper loops and impairments.

II. Discrete Multitone (DMT) Modulation

Discrete multitone (DMT) modulation divides a channel into a set of parallel independent subchannels. The SNR of each subchannel is measured and an appropriate amount of information or bits is then assigned to each subchannel. As a result, the DMT system optimizes performance for any channel that it encounters, by virtue of the adaptive, selective bit/information allocation to each of the independent subchannels. Fig. 1 shows the basic structure of DMT systems. At the transmitter, the data is modulated by a set of parallel, independent subchannels, $p_i, i = 0, \cdots, N_c - 1$, where N_c is the number of independent subchannels. The $p_i s$ divide up the channel and modulate the input data, $x_i, i = 0, \cdots, N_c - 1$. The modulated signal is then summed together before it is sent to the channel, h_k. At the receiver, the received signal is demodulated by the corresponding set of demodulating vectors that separate the received signal into a set of parallel, independent subchannels.

A specific implementation of the DMT system is shown in Figs. 2 and 3. The modulation and demodulation techniques we used are the inverse fast Fourier transform (IFFT) and the fast Fourier transform (FFT), respectively. Efficient algorithms for IFFT and FFT are well-known and thus significantly reduce the complexity of implementing the modulation and demodulation functions.

The binary input data are parsed onto a set of parallel, independent subchannels, each of which is assigned a fixed number of bits during startup or system initialization. Given the measured SNR of each subchannel during startup, the number of bits for each subchannel is then determined. Each subchannel is encoded into a QAM constellation of the appro-

priate size. For example, if four bits are assigned to tone i, then tone i will use a 16-QAM constellation for encoding. Optional coding can be inserted as shown in the encoder block in Fig. 2. The modulation function, IFFT, converts the encoded binary data in QAM constellation format from frequency domain to time domain signal for transmission. The demodulation function (FFT) at the receiver reverts the time domain signal back to frequency domain data.

The DMT system described in [5] and shown in Figs. 2 and 3 also contains a guard band in the form of cyclic prefix. The length of the cyclic prefix determines the amount of the guard band. As long as the inter-symbol interference (ISI) of the channel is not longer than the length of the cyclic prefix, then the use of the cyclic prefix results in DMT symbols that are free of inter-block interference (IBI).

A potential problem in the implementation of the DMT modulation methods is the use of the cyclic prefix of an extra ν samples, where $\nu+1$ is the length in sampling periods of the channel pulse response [6]. The required overhead with respect to the data rate is then $\nu/(N_c+\nu)$. On many practical channels including the high-speed subscriber loop, ν can be large. To minimize the data rate loss due to the overhead, N_c needs to be very large, potentially 10 000 samples or more. Complexity is still minimal with the DMT methods with large N_c, when measured in terms of operation per unit time interval. However, large N_c implies large memory requirement to store the bit allocation tables and intermediate FFT/IFFT results, often dominating the implementation complexity. Further, large N_c implies longer latency in processing. Long latency can create problems with synchronization and can also be unacceptable with certain higher-level data protocols.

One solution to the latency problem is to use a combination of short-length equalization and the DMT to reduce ν, and thereby the required N_c, to reach the highest performance levels with less memory and less latency. The equalizer used is known as a time-domain equalizer (TEQ).

At the receiver front-end, the TEQ, $w(D)$, in the form of a $(M+1)$-tap FIR filter is performed (as shown in Fig. 3). This TEQ shortens the channel response so that the combined response of the channel and the TEQ taps is limited to a small number of samples, ideally equal to or less than the length of the cyclic prefix. Following the TEQ, the cyclic prefix samples are removed from the equalized signal. The remaining equalized time-domain samples, $z_k, k = 0, 1, \cdots, N_c - 1$, are then demodulated by the N_c-point FFT function to frequency-domain data, resulting in $N_c/2$ complex subsymbols. Appropriate gain and phase adjustment in the form of a set of $N_c/2$ 1-tap complex LMS filters $(A_n, n = 0, 1, \cdots, N_c/2 - 1)$ are multiplied to the demodulated signal $(Z_n, n = 0, 1, \cdots, N_c/2 - 1)$ before symbol decision and decoding. If the optional trellis coding is used at the transmitter, then a corresponding Viterbi will be added at the receiver.

The TEQ and cyclic prefix for the DMT system are analogous to the feedforward taps and the feedback taps of a DFE system. Both the TEQ of a DMT system and the feedforward taps of a DFE system are FIR filters. The feedback taps of a DFE system are equal to the combined channel and feedforward FIR response. The length of the feedback filter is the same as the length of the cyclic prefix in terms of the functionality.

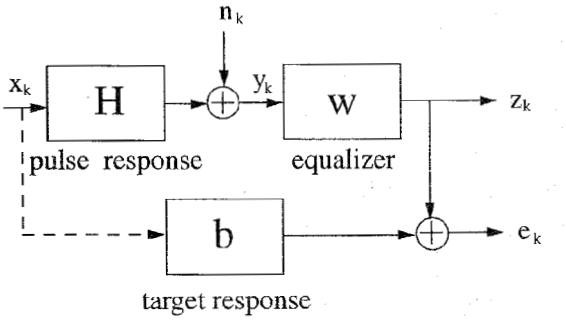

Fig. 4. Structure of the TEQ.

Reference [2] suggests a method to compute the TEQ taps. However, this method requires matrix inversion computation and often results in fairly high cost of implementation, especially for cases of large size FFT. An alternative method is proposed in [3] that requires far less complexity. The method in [3] starts with specifying the number of FIR taps for the TEQ and the length of the cyclic prefix. It then iterates until a suitable criterion is satisfied. The drawback of this method is the length of time it takes to obtain a good set of TEQ taps. Even though the TEQ training is performed only once during startup or initialization, there are applications where a short startup time is critical.

Thus in Section IV, we will show a fast training algorithm that has less complexity than the method described in [2] and requires less training time than the method described in [3].

III. Equalizer Settings for the TEQ

The structure of the TEQ is described in Fig. 4. The goal of the TEQ is to reduce the size of the cyclic prefix so that the overall data rate loss is minimized. The TEQ uses the feedforward filter $\boldsymbol{w}$ to shape the channel to the target response $\boldsymbol{b}$ with a short length. There are several criteria that can be applied to the target response. In this paper, we put a unit tap constraint on $\boldsymbol{b}$ so that one of $\boldsymbol{b}$ tap is set to 1. Actually, the TEQ proposed in [2] subsumes the DFE since the feedback filter in the DFE (corresponding to the target response in the TEQ) is restricted to being monic. With a unit tap constraint, the TEQ chooses the optimum settings $\boldsymbol{w}$ and $\boldsymbol{b}$ that minimize the mean square error.

Assuming that the pulse response $h(t)$ extends over a finite interval $0 \le t \le \nu T$, where T denotes the symbol period, with a symbol-spaced equalizer, the input/output relation for the discrete time equivalent channel has the form

$$y_k = \sum_{m=0}^{\nu} h_m x_{k-m} + n_k$$

where $\{y_k\}$ is the channel output sequence, $\{h_k\}$ is the channel pulse response, $\{x_k\}$ is the channel input sequence with signal power $\bar{\varepsilon}_x$, and $\{n_k\}$ is the additive Gaussian noise sequence with variance σ_n^2. We assume that the channel input sequence $\{x_k\}$ and the noise sequence $\{n_k\}$ are uncorrelated with each other. In typical high-speed subscriber loop, the noise sequence is colored due to crosstalk.

From the above equation, we can form the following relation:

$$\boldsymbol{y}_k = H\boldsymbol{x}_k + \boldsymbol{n}_k$$

where

$$\boldsymbol{y}_k = \begin{bmatrix} y_k \\ y_{k-1} \\ \vdots \\ y_{k-M+1} \end{bmatrix}, \quad \boldsymbol{x}_k = \begin{bmatrix} x_k \\ x_{k-1} \\ \vdots \\ x_{k-M-\nu+1} \end{bmatrix},$$

$$\boldsymbol{n}_k = \begin{bmatrix} n_k \\ n_{k-1} \\ \vdots \\ n_{k-M+1} \end{bmatrix},$$

and

$$H = \begin{bmatrix} h_0 & h_1 & \cdots & h_\nu & 0 & \cdots & 0 \\ 0 & h_0 & h_1 & \cdots & h_\nu & \cdots & \\ \vdots & \vdots & \ddots & \ddots & \ddots & \ddots & \vdots \\ 0 & \cdots & 0 & h_0 & h_1 & \cdots & h_\nu \end{bmatrix}.$$

We will denote the feedforward filter and the target response by $\boldsymbol{w}$ and $\boldsymbol{b}$, where $\boldsymbol{w} = [w_0 w_1 \cdots w_{M-1}]^T$ and $\boldsymbol{b} = [b_0 b_1 b_2 \cdots b_{N-1}]^T$. Thus, the lengths of the feedforward filter and the target response are M and N, respectively. Also, from the above equation, we define $R_{xx} = E[\boldsymbol{x}_{k-\Delta}\boldsymbol{x}_{k-\Delta}^*]$, $R_{xy} = R_{yx}^* = E[\boldsymbol{x}_{k-\Delta}\boldsymbol{y}_k^*]$ and $R_{yy} = E[\boldsymbol{y}_k\boldsymbol{y}_k^*]$ where Δ represents the decision delay.

From the figure, the error is defined as

$$e_k = \boldsymbol{b}^T\boldsymbol{x}_{k-\Delta} - \boldsymbol{w}^T\boldsymbol{y}_k$$

where $\boldsymbol{x}_{k-\Delta} = [x_{k-\Delta}x_{k-\Delta-1}\cdots x_{k-\Delta-N+1}]^T$.

Then, from the orthogonality principle, the desired target response in the TEQ [2] is

$$\boldsymbol{b} = \frac{\boldsymbol{R}_{x|y}^{-1}\boldsymbol{e}_l}{\boldsymbol{e}_l^T\boldsymbol{R}_{x|y}^{-1}\boldsymbol{e}_l} \tag{1}$$

where

$$\boldsymbol{R}_{x|y} = \boldsymbol{R}_{xx} - \boldsymbol{R}_{xy}\boldsymbol{R}_{yy}^{-1}\boldsymbol{R}_{yx}$$

and $\boldsymbol{e}_l$ is the unit column vector with 1 in lth position. Also, the feedforward filter (the TEQ taps [2]) is

$$\boldsymbol{w} = \boldsymbol{R}_{yy}^{-1}\boldsymbol{R}_{yx}\boldsymbol{b}. \tag{2}$$

The optimal $\boldsymbol{b}$ and $\boldsymbol{w}$ are determined by searching for all possible l $(0 \le l \le N-1)$ to maximize the achievable data rate in the DMT system.

It is straightforward to check that with $l = 0$ the above solutions equal to the DFE solution. Since the DFE solution is a subset of the TEQ solution, it is easy to extend the fast algorithm for the DFE in [1] to one for the TEQ settings. In the following section, we briefly revisit the fast algorithm and derive one for the TEQ in a colored noise channel.

IV. A Fast Equalization Algorithm

This section illustrates the fast algorithm for the TEQ in a symbol-spaced case with a colored noise.

Using the fact that a circulant matrix has the discrete Fourier transform basis vectors as its eigenvectors, and the discrete Fourier transform of its first column as its eigenvalues [4], an M by M circulant matrix $\boldsymbol{C}$ can be decomposed as

$$\boldsymbol{C} = \frac{1}{M}\boldsymbol{P}^*\Lambda_C\boldsymbol{P}$$

where $\boldsymbol{P}$ is the discrete Fourier transform (DFT) matrix with

$$p_{m,n} = e^{-j2\pi mn/M}, \qquad 0 \le m,n \le M-1$$

and $\Lambda_C = \operatorname{diag}[C_0, C_1, \cdots C_{M-1}]$ is the diagonal matrix whose diagonal element C_i is the ith element of the M-point DFT of the first column of the circulant matrix $\boldsymbol{C}$. It is useful to partition P into P_1 and P_2: $P = [\boldsymbol{P}_1\boldsymbol{P}_2]$ where the sizes of $\boldsymbol{P}_1$ and $\boldsymbol{P}_2$ are M by N and M by $M-N$ respectively.

In the fast algorithm, we assume that the feedforward filter $\boldsymbol{w}$ is longer than the target response $\boldsymbol{b}$ $(M \ge N)$. This restriction may not be practical in some subscriber loop, where the target response can be longer than the feedforward filter. However, a long feedforward filter can be accurately approximated by a pole-zero filter with fewer coefficients using a computationally-efficient algorithm described in [7] with little performance loss.

More detailed derivation is found in [1]. Similarly, it is easy to see that in a colored noise case, the Toeplitz autocorrelation matrices are approximated to the circulant matrices:

$$\boldsymbol{R}_{yy} = \frac{1}{M^2}\boldsymbol{P}^*\Lambda_{\overline{\varepsilon}_x M|H|^2+|\tilde{N}|^2}\boldsymbol{P}$$

and

$$\boldsymbol{R}_{yx} = \frac{1}{M}\boldsymbol{P}^*\Lambda_{\overline{\varepsilon}_x H^* P_\Delta}\boldsymbol{P}_1$$

where H_i is ith element of M-point DFT of $[h_0, h_1, \cdots h_\nu, 0, \cdots 0]$, $\tilde{N}_i$ is the ith element of the DFT of $[n_{M-1}, n_{M-2}\cdots n_0]$ and $p_{\Delta,i} = e^{-j2\pi\Delta i/M}$.

Substituting the above equations into equations in the previous section yields

$$\boldsymbol{R}_{x|y} = \frac{1}{M}\boldsymbol{P}_1^*\Lambda_{\frac{\overline{\varepsilon}_x|\tilde{N}|^2}{\overline{\varepsilon}_x M|H|^2+|\tilde{N}|^2}}\boldsymbol{P}_1$$

and

$$\boldsymbol{R}_{yy}^{-1}\boldsymbol{R}_{yx} = \boldsymbol{P}^*\Lambda_{\frac{\overline{\varepsilon}_x H^* p_\Delta}{\overline{\varepsilon}_x M|H|^2+|\tilde{N}|^2}}\boldsymbol{P}_1.$$

We note that $R_{x|y}$ is an N by N upper left submatrix of a circulant matrix whose first column is the inverse DFT of $\frac{\overline{\varepsilon}_x|\tilde{N}|^2}{\overline{\varepsilon}_x M|H|^2+|\tilde{N}|^2}$.

It can be shown that using the Schur complement,[1] the inverse of $\boldsymbol{R}_{x|y}$ is

$$\left(\frac{1}{M}\boldsymbol{P}_1^*\Lambda_{X|Y}\boldsymbol{P}_1\right)^{-1} = \frac{1}{M}\boldsymbol{P}_1^*\Lambda_{X|Y}^{-1}\boldsymbol{P}_1 - \frac{1}{M}\boldsymbol{P}_1^*\Lambda_{X|Y}^{-1} \cdot \boldsymbol{P}_2(\boldsymbol{P}_2^*\Lambda_{X|Y}^{-1}\boldsymbol{P}_2)^{-1}\boldsymbol{P}_2^*\Lambda_{X|Y}^{-1}\boldsymbol{P}_1$$

where $\Lambda_{X|Y} = \Lambda_{\frac{\overline{\varepsilon}_x|\tilde{N}|^2}{\overline{\varepsilon}_x M|H|^2+|\tilde{N}|^2}}$.

[1] The Schur complement of $\boldsymbol{D}$ in the block matrix $\begin{bmatrix} \boldsymbol{A} & \boldsymbol{B} \\ \boldsymbol{C} & \boldsymbol{D} \end{bmatrix}$ is $\boldsymbol{A} - \boldsymbol{C}\boldsymbol{D}^{-1}\boldsymbol{B}$ [8].

Neglecting the last term of the right hand side in the above equation, $\boldsymbol{R}_{x|y}^{-1}$ is approximated by

$$\boldsymbol{R}_{x|y}^{-1} = \frac{1}{M}\boldsymbol{P}_1^*\Lambda^{-1}_{\frac{\overline{\varepsilon}_x|\tilde{N}|^2}{\overline{\varepsilon}_x M|H|^2+|\tilde{N}|^2}}\boldsymbol{P}_1 = \frac{1}{\overline{\varepsilon}_x M}\boldsymbol{P}_1^*\Lambda_{\frac{\overline{\varepsilon}_x M|H|^2}{|\tilde{N}|^2}+1}\boldsymbol{P}_1.$$

Note that when $\boldsymbol{w}$ and $\boldsymbol{b}$ have the same length ($M = N$), $\boldsymbol{R}_{x|y}^{-1}$ is exactly $(1/M)\boldsymbol{P}^*\Lambda_{X|Y}^{-1}\boldsymbol{P}$ and no approximation takes place. Plugging the above equation into (1) yields

$$\begin{aligned}\boldsymbol{b} &= \frac{1}{k}\frac{1}{\overline{\varepsilon}_x M}\boldsymbol{P}_1^*\Lambda_{\frac{\overline{\varepsilon}_x M|H|^2}{|\tilde{N}|^2}+1}\boldsymbol{P}_1\boldsymbol{e}_l \\ &= \frac{1}{k'}\boldsymbol{P}_1^*\Lambda_{\frac{\overline{\varepsilon}_x M|H|^2}{|\tilde{N}|^2}+1}\boldsymbol{p}_l \\ &= \frac{1}{k'}[I0]\boldsymbol{P}^*\begin{bmatrix}\mathrm{SNR}_0+1\\(\mathrm{SNR}_1+1)e^{-j2\pi l/M}\\\vdots\\(\mathrm{SNR}_{M-1}+1)e^{-j2\pi(M-1)l/M}\end{bmatrix}\end{aligned}$$

where k' is a scaling constant to make the lth element of the target response $\boldsymbol{b}$ equal to 1 ($b_l = 1$), $\boldsymbol{p}_l$ is the l the column of $\boldsymbol{P}$, I is the N by N identity matrix and $\mathrm{SNR}_i = \frac{\overline{\varepsilon}_x M|H_i|^2}{|\tilde{N}_i|^2}$.

Then, defining $\overline{B}_i$ as

$$\overline{B}_i = \frac{1}{k'}(\mathrm{SNR}_i+1)e^{-j2\pi il/M}, \qquad i = 0, 1\cdots M-1,$$

the target response can be obtained from the IDFT operation:

$$b_k = \frac{1}{M}\sum_{i=0}^{M-1}\overline{B}_i e^{j2\pi ik/M}, \qquad k = 0, 1, \cdots N-1.$$

With $\boldsymbol{b}$, we can compute the feedforward filter $\boldsymbol{w}$ from (2):

$$\boldsymbol{w} = \boldsymbol{P}^*\Lambda_{\frac{\overline{\varepsilon}_x H^* p_\Delta}{\overline{\varepsilon}_x M|H|^2+|\tilde{N}|^2}}\boldsymbol{P}\begin{bmatrix}\boldsymbol{b}\\0\end{bmatrix}.$$

Then, multiplying both sides by $\boldsymbol{P}$ yields

$$W_i = \frac{\overline{\varepsilon}_x M H_i^* p_{\Delta,i}\cdot B_i}{\overline{\varepsilon}_x M|H_i|^2+|\tilde{N}|^2}, \qquad i = 0, 1, \cdots M-1$$

where W_i is the ith DFT element of $\boldsymbol{w}$ and B_i is the ith M-point DFT element of $[b_0 b_1 \cdots b_{N-1}0\cdots 0]$.

From this equation, we can obtain w_k using the IDFT:

$$w_k = \frac{1}{M}\sum_{i=0}^{M-1}W_i e^{j2\pi ik/M}, \qquad k = 0, 1, \cdots M-1.$$

Using the above DFT and IDFT operations, the computation of the TEQ coefficients are carried out very efficiently. We have found in [1] that calibrating $\boldsymbol{b}$ by a scaling factor α yields a better solution. The equation for the optimum α has been derived in [1].

As explained in [1], the solution from the fast algorithm converge to the optimal solution as M increases, since the approximation of a Toeplitz matrix by a circulant matrix becomes accurate as the size of a matrix grows. This will be verified through simulations later.

In summary, we compute the TEQ settings for each l value and pick the optimum settings to achieve the highest throughput in the DMT system. After the TEQ coefficients are obtained using the fast algorithm, the LMS algorithm may be employed for the tracking purpose afterwards.

V. Channel Identification

In this section, we briefly analyze the channel identification method that the proposed fast algorithm can adopt.

There are several schemes that carry out the channel identification efficiently. Channel identification methods measure the channel pulse response assuming the noise spectrum is flat. The channel noise is an undesired disturbance in channel pulse response estimation, and this noise needs to be averaged in determining the channel response.

One easy method is to use a periodic training sequence x_k with period M, equal to or slightly longer than the length of the channel pulse response. The receiver measures the corresponding channel output averaging over L cycles, and then divides the DFT of the channel output by the DFT of the known training sequence. The channel estimate in the frequency domain is

$$\hat{H}_n = \frac{1}{L}\sum_{i=1}^{L}\frac{Y_{i,n}}{X_n}$$

where $Y_{i,n}$ is the nth element of the DFT of the channel output on ith cycle and X_n is the nth element of the DFT of the input training sequence.

It can be shown [6] that the overall MSE of the estimation error is equal to $(1+1/L)\sigma_n^2$ where σ_n^2 is the power of the additive noise. The excess MSE then has variance $(1/L)\sigma_n^2$ that is reduced by a factor equal to the number of averaging. Therefore, when $L = 40$, we can tolerate only $1+\frac{1}{40} = 0.1$ dB excess error in channel pulse response estimation. Even considering the worst channel pulse response in typical subscriber loops (in terms of the length of the channel memory), with total 5000 sample periods an accurate pulse response estimation can be carried out resulting in less than 0.1 dB excess MSE. Combining this channel estimation scheme, the proposed fast algorithm still produce the equalizer settings very efficiently in contrast to the traditional recursive adaptive algorithm.

In the following section, simulation results using the fast algorithm are shown.

VI. Simulations

This section presents simulation results using the fast algorithm described in the previous section and compares them with the optimal TEQ settings obtained by a direct matrix inversion. A symbol-spaced equalizer is assumed in this simulation. Also the optimized α is used to scale $\boldsymbol{b}$. To simplify the analysis in simulations, we restrict l to 0. Also, instead of the data rate, $\mathrm{SNR} = \overline{\varepsilon}_x/E[|e_k|^2]$ is used as a performance measure to indicate the performance of the fast algorithm.

Several length copper loops with 26 gauge have been used for simulations. Matched filter bound (MFB) $\mathrm{SNR}_{\mathrm{MFB}} = ||h||^2\overline{\varepsilon}_x/\sigma_n^2$ is set to 20 dB throughout this study, if not stated

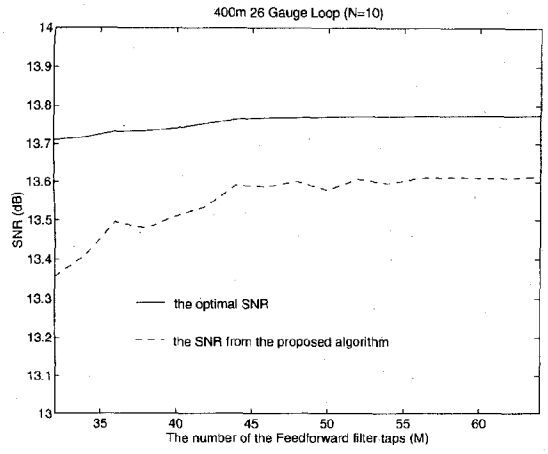

Fig. 5. Performance of the proposed algorithm with different feedforward filter length.

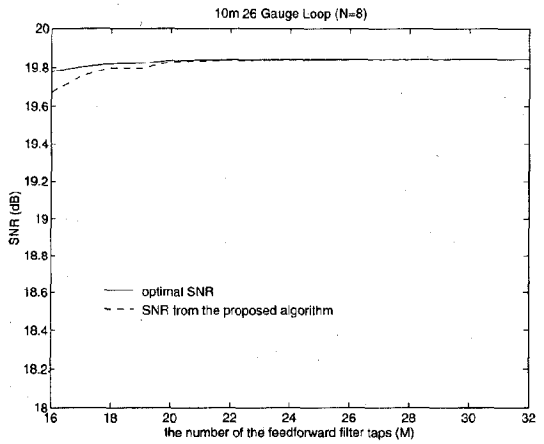

Fig. 6. Performance of the proposed algorithm with different feedforward filter length.

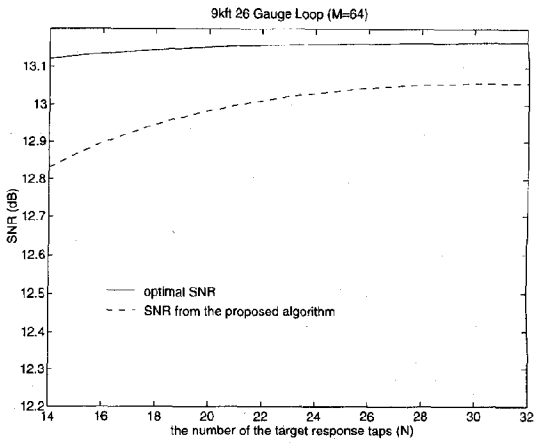

Fig. 7. Performance of the proposed algorithm with different target response length.

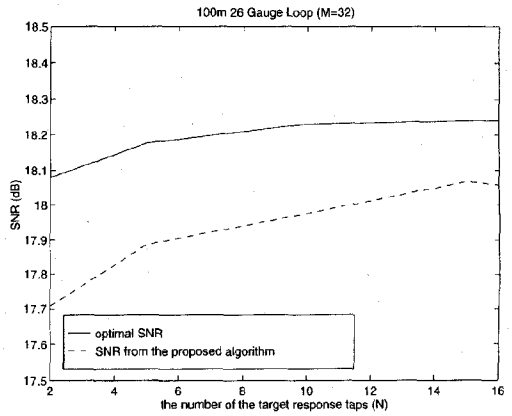

Fig. 8. Performance of the proposed algorithm with different target response length.

otherwise. In the plots, the solid line represents the optimal SNR computed from the direct matrix inversion and the dashed line indicates the SNR computed from the fast algorithm.

1) Length of the Feedforward Filter: In Figs. 5 and 6, the number of the feedforward filter taps (M) is changed for a 26 gauge 400 m and a 10 m loop, respectively. For each simulations, the lengths of the target response are set to 8 and 10. It is obvious that as the length of the feedforward filter increases, performance of the proposed algorithm approaches that of the optimal TEQ coefficients within a tenth of a dB. In a shorter loop, the proposed algorithm works better. As shown in Fig. 6, with feedforward filters longer than 20 taps, the gap between the optimal settings and the coefficients obtained from the fast algorithm becomes indiscernible.

2) Length of the Target Response: We performed the fast algorithm on 26 gauge 9 kft and 100 m loop in Figs. 7 and 8 with various choices of the target response length. For simulation, the length of the feedforward filter is set to an integer power of 2 (64 and 32 in Figs. 7 and 8, respectively) so that the DFT operations are carried out by the fast Fourier transform (FFT) to speed up the computation. Nine kft 26 gauge loop channel is used as an example for ADSL loop, since this loop represents one of the worst case loops among the set of CSA loops [9]. For both cases, the proposed algorithm generates near-optimal solutions.

3) Transmit Power: We changed the transmit power in 400 m 26 gauge loop. Fig. 9 shows the performance of the proposed algorithm from MFB = 10–30 dB. The lengths of the feedforward filter and target response are set to 64 and 18, respectively. Simulation indicates the fast algorithm generates solutions close to the optimum settings consistently regardless of the transmit power.

4) Crosstalk Coupling: The near-end crosstalk (NEXT) term is modeled [10] with a coupling function of the form: $|H_{\mathrm{NEXT}}(f)|^2 = K_{\mathrm{NEXT}} f^{3/2}$, where f is the frequency in Hz and K_{NEXT} is determined through empirical measurement. In this simulation, the far-end crosstalk (FEXT) is assumed to be negligible because we consider short loops here. We changed K_{NEXT} from 10^{-15} to 10^{-13} in 400 m 26 gauge loop and the fast algorithm in a colored noise case is used for simulation. In this simulation, an input signal power of 10 mW and a noise power of -30 dBm across a two-sided bandwidth are assumed. As the effect of the near-end crosstalk increases, the output SNR decreases in Fig. 10. Again, the SNR from the proposed fast algorithm is only a few tenth of a dB away

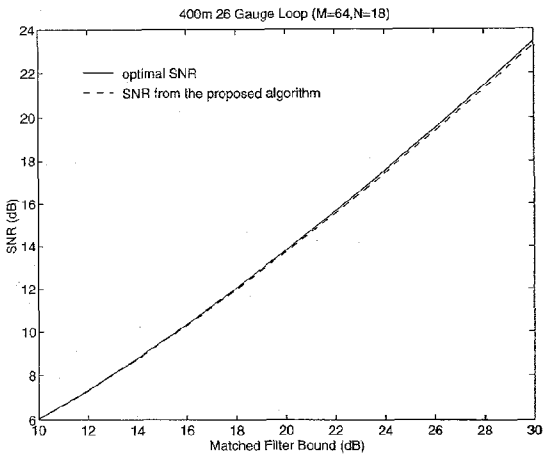

Fig. 9. Performance of the proposed algorithm with different MFB.

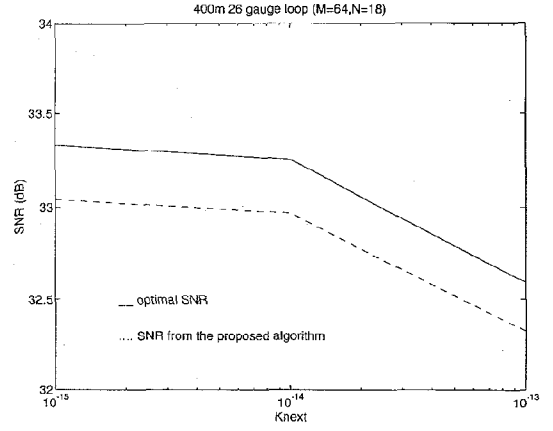

Fig. 10. Performance of the proposed algorithm with different K_{next}.

from the optimum solution in a subscriber loop corrupted by the near-end crosstalk.

Our performance evaluations showed that the proposed algorithm performs very well in various situations. The gap between the optimal SNR and the SNR from the proposed algorithm is shown to be a few tenths of a dB and becomes negligible as the length of the feedforward filter increases. Thus, for any sufficiently long feedforward filter, the proposed algorithm can compute the optimal equalizer setting very efficiently without any performance loss.

VII. Conclusion

We have illustrated a fast algorithm for the time-domain equalizer (TEQ) in the discrete multitone (DMT) modulation for high performance copper networks. The overall computation is carried out with negligible performance loss as the number of the feedforward filter taps increases.

Simulations have been performed in various copper loop channels. Effects of the feedforward and target response length, the matched filter bound and the near-end crosstalk coupling have been examined. Simulation results show that the fast algorithm yields near-optimal settings very efficiently in various environments.

References

[1] I. Lee and J. M. Cioffi, "A fast computation algorithm for the decision feedback equalizer," *IEEE Trans. Commun.*, vol. 43, no. 11, pp. 2742–2749, Nov. 1995.
[2] J. Chow and J. M. Cioffi, "A cost effective maximum likelihood receiver for multicarrier systems," in *Proc. ICC*, 1992.
[3] J. Chow, J. M. Cioffi, and J. A. Bingham, "Equalizer training algorithms for multicarrier modulation systems," presented at *ICC*, 1993.
[4] R. Gray, "On the asymptotic eigenvalue distribution of Toeplitz matrices," *IEEE Trans. Inform. Theory*, vol. IT-18, pp. 725–730, Nov. 1972.
[5] J. S. Chow, J. C. Tu, and J. M. Cioffi, "A discrete multitone transceiver system for HDSL applications," *IEEE J. Select. Areas Commun.*, vol. 9, pp. 895–908, Aug. 1991.
[6] J. M. Cioffi, *EE 479 Course Notes*. Stanford: Stanford Univ., 1994.
[7] N. Al-Dhahir, A. Sayed, and J. Cioffi, "A high performance cost-effective pole-zero MMSE-DFE," in *Allerton Conf. Commun., Control and Computing*, 1993, pp. 1166–1175.
[8] T. Kailath, *Linear Systems*. Englewood Cliffs, NJ: Prentice-Hall, 1980.
[9] P. S. Chow, J. C. Tu, and J. M. Cioffi, "Performance evaluation of a multichannel transceiver system for ADSL and VHDSL services," *IEEE J. Select. Areas Commun.*, vol. 9, pp. 909–919, Aug. 1991.
[10] D. G. Messerschmitt, "Design issues in the ISDN U-interface transceiver," *IEEE J. Select. Areas Commun.*, vol. SAC-4, pp. 1281–1293, 1986.

Inkyu Lee (S'91) was born in Seoul, Korea, on December 26, 1967. He received the B.S. degree in control and instrumentation engineering from Seoul National University, Seoul, Korea, in 1990. He received the M.S. and Ph.D. degrees in electrical engineering from Stanford University, Stanford, CA, in 1992 and 1995, respectively.

From 1991 to 1995, he was a research assistant at the Information Systems Laboratory at Stanford University. His current research interests include digital communications and signal processing techniques applied to digital transmission and storage systems.

Jacky S. Chow (S'86–M'93) received the B.S. degree in electrical engineering (summa cum laude) from California State University, Fresno, in 1987, and the M.S. and Ph.D. degrees in electrical engineering from Stanford University, Stanford, CA in 1988 and 1992, respectively.

He joined Amati Communications Corporation, CA, in 1992, and is currently a Program Manager. He specialized in developing multicarrier transceiver systems for various coding, digital signal processing, algorithms, and VLSI system optimization and implementation.

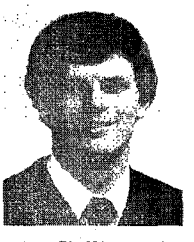

John M. Cioffi (S'77–M'78–SM'91) received the B.S.E.E. degree from Illinois University, in 1978, and the Ph.D. and E.E. degrees from Stanford University, in 1984.

He was employed by Bell Laboratories, Holmdel, NJ, from 1978 to 1984, and by IBM Research, San Jose, CA, from 1984 to 1986. He has been on the Stanford faculty since 1986 and is now Chief Technical Officer at Amati Communications Corp, a company he founded in 1990. His interests are in data transmission and storage.

Dr. Cioffi's was the recipient of the 1991 IEEE Communications Magazine prize paper award and was a National Science Foundation Presidential Investigator from 1987 to 1992.